Materials Transactions, Vol. 50, No. 1 (2009) pp. 96 to 100
Special Issue on Severe Plastic Deformation for Production of Ultrafine Structures and Unusual Mechanical Properties: Understanding Mechanisms
©2009 The Japan Institute of Metals

Microstructure Evolution in Pure Al Processed with Twist Extrusion

Dmitry Orlov[1], Yan Beygelzimer[2], Sergey Synkov[2], Viktor Varyukhin[2], Nobuhiro Tsuji[1] and Zenji Horita[3]

[1]*Department of Adaptive Machine Systems, Graduate School of Engineering, Osaka University, Suita 565-0871, Japan*
[2]*Department of Physics of High Pressures and Advanced Technologies, Donetsk Institute for Physics & Engineering of the National Academy of Sciences–Ukraine, 72 R. Luxembourg St., Donetsk, 83114, Ukraine*
[3]*Department of Materials Science and Engineering, Faculty of Engineering, Kyushu University, Fukuoka 819-0395, Japan*

High purity Al (99.99%) was subjected to severe plastic deformation through twist extrusion at room temperature. Microstructures were examined for 1 pass and 4 passes on the cross section perpendicular to the longitudinal axis of billets using optical microscopy and electron back scatter diffraction analysis. It was shown that a vortex-like material flow was observed on the cross section and this became more intense with increasing number of the pressing. After one pass, subgrain structures with low angle grain boundaries were developed throughout the section but after 4 passes, the microstructure consisted of grains surrounded by high angle boundaries with fraction of ~70% in the edge parts. The average grain size at the edge parts is refined to ~1.6 μm. [doi:10.2320/matertrans.MD200802]

(Received April 18, 2008; Accepted July 28, 2008; Published September 10, 2008)

Keywords: *aluminum, twist extrusion, severe plastic deformation, optical microscopy, electron backscattered diffraction (EBSD)*

1. Introduction

Recently, scientists and engineers are very much attracted to nano- and ultrafine-grained (UFG) materials because of their unique structures and properties.[1–3] Special attention is paid to the process of severe plastic deformation (SPD) since it allows to produce UFG materials in bulk forms.[2] Many SPD processes are available now, such as high pressure torsion (HPT),[4] equal-channel angular pressing (ECAP),[5,6] multiple forging,[7] repetitive corrugation and straightening,[8] accumulative-roll bonding (ARB),[9,10] and twist extrusion (TE).[11,12]

The TE process was first introduced by Beygelzimer *et al.*[11–14] and related works have been published thereafter.[15–17] In TE, a billet is pressed through an extrusion die whose cross section remains unchanged, while the billet is twisted with an angle β about its longitudinal axis as illustrated in Fig. 1. The billet maintains its size and shape of the cross section after each TE pass. Thus it is possible to repeat the pressing to accumulate a large strain and to attain grain refinement as other SPD processes. The TE process can be applicable for any samples except having circular cross section. Main parameters affecting plastic flow (and, accordingly, accumulated strain value and distribution) in TE are shape of the twist channel cross-section, the twisting angle θ, height h and slope angle β of the twist part of the channel (see Fig. 1). In more details features of the twist extrusion techniques has been described in,[16] and strain estimation in TE is shown in the next section.

TE has been used for grain refinement of pure Cu of a commercial grade,[16] titanium[18–20] and Al-based alloys.[15,17] Nevertheless, there seems no systematic experiment so far for microstructure analysis in TE-processed billet. It may be useful to understand macro flow patterns in TE using physical and mathematical modeling. However, further study for microstructure evolution is also needed for experimental verification on real metallic systems. In this study, pure polycrystalline Al is adopted to TE as it is the most representative metallic system having fcc crystal structure. TE processed pure Al has been well studied in terms of both macro- and microstructure to obtain much information for comparison with the data from other SPD processes.[21–24]

2. Experimental

This study used a high purity 99.99% aluminum produced by ingot casting. Edge parts and 2 mm surface layers of the as-received ingot were machined out. The ingot was hydro-extruded at room temperature to a billet with cross-sectional dimensions of $18 \times 28\,\mathrm{mm}^2$ and it was cut to length of 100 mm for TE. The billets were annealed at 500°C for 1 hour and cooled in furnace.

TE was conducted at room temperature with the extrusion speed of $\sim 3\,\mathrm{mm \cdot s^{-1}}$ using a twisting die having $\beta = 60°$. A backpressure of ~200 MPa was applied to the billets during TE. According to Ref. 12), net strain in twist extrusion has distribution within cross-section of the billet so that minimal ($\varepsilon_{\min}$) and maximal ($\varepsilon_{\max}$) strain accumulated in a billet after one TE pass could be estimated by simplified equations:

$$\varepsilon_{\min} \approx 0.4 + 0.1 \tan\beta; \quad (1)$$

$$\varepsilon_{\max} \approx \frac{2}{\sqrt{3}} \tan\beta. \quad (2)$$

More details of strain distribution after 1 TE pass are found elsewhere.[12,15,25] For the tool parameters used in this study, average true strain of $\varepsilon_{ave} \approx 1.2$ was introduced for a single pass.[12] This level of strain is comparable to strain introduced in a billet after 1 ECAP pass through 90° channel intersection die or 70% reduction in rolling. The twist extrusion was repeated up to 4 passes which come to a total average strain of $\varepsilon_{ave} \approx 4.8$.[12] This level of strain may be sufficient to attain UFG structures by ECAP[22] or ARB.[21]

In our earlier study,[25] TEM observations and microhardness data of this investigation have been reported. The present report is mostly concentrated on analysis of structure evolution through optical microscopy and Electron Back-

Table 1 Total accumulated strain calculated by equations from Ref. 12) related to fractions of HABs and (sub)grain sizes at positions A and B after 1 and 4 TE passes.

Specimen state, position		Equivalent strain		Fractions of HABs,	(sub)grain size,
		average	local	[%]	[μm]
1 pass	Point A	1.2	0.6	7.6	3.16
	Point B		2	14.5	3.08
4 passes	Point A	4.8	2.4	53	1.88
	Point B		8	71	1.61

scattered Diffraction (EBSD) analysis. Optical microscopy was undertaken using Nikon ECLIPSE ME600L equipped with a digital camera to observe material flow patterns in the billets before and after TE. Electron backscatter diffraction (EBSD) analysis was also conducted using Hitachi S-4300SE equipped with a field emission gun at an accelerating voltage of 30 kV. Imaging of crystal orientation using EBSD involved automatic beam scanning with step sizes of 0.08–0.3 μm. Grain sizes and misorientation angles were determined along with the EBSD analysis. Data acquisition and subsequent analysis were performed using a TSL orientation image microscopy system. A cleaning-up procedure was applied to all EBSD images to adjust points with confidence index lower than 0.1. It is noted that, for all the EBSD maps scanned, average confidence index was >0.3. Misorientations less than 2° were excluded from the analysis because of the limitations of the angular resolution of the EBSD technique.[26] Thus, low angle boundaries (LABs) were defined as those having misorientations from 2° to 15° and high angle boundaries (HABs) as having misorientations greater than 15°.

Specimens for optical microscopy were cut by an abrasive saw and mechanically ground by abrasive papers. They were anodized in a solution containing 5% HBF_4 in H_20 at room temperature with a voltage of ~20 V. For EBSD analysis, the samples were electro-polished in a perchloric-based solution at room temperature with a voltage of ~12 V. Special attention was paid to define directions of the samples with respect to the billet geometry as illustrated in Fig. 1, where the extrusion direction (ED) is parallel to the longitudinal axis of the billet and the normal direction (ND) and transverse direction (TD) are, respectively, parallel to the short and long axes on the cross-sectional plane perpendicular to ED of the billet. EBSD analysis was conducted at points marked A and B in Fig. 1, which represents minimal and maximal strain values, respectively (see Table 1).

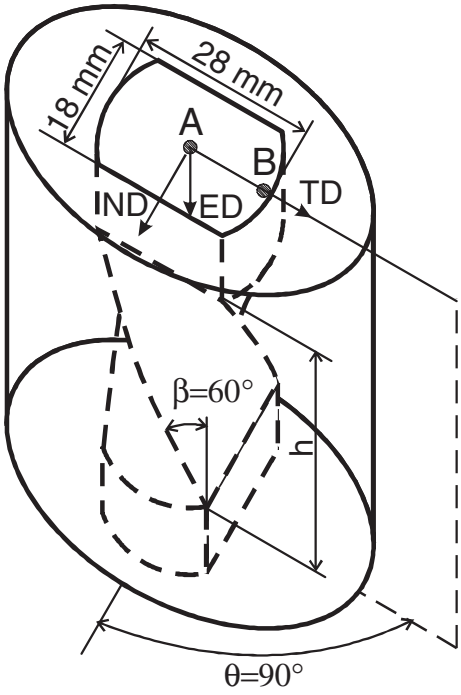

Fig. 1 Illustration of die for twist extrusion showing the channel dimensions, definition of directions and points of observations.

3. Results and Discussion

After annealing of the hydrostatically extruded billet, the microstructure consists of different sizes of recrystallized grains as shown in Fig. 2(a). It appears that the sizes of individual grains vary over one order of magnitude. EBSD analysis showed that the average grain size was ~280 μm.

Figure 2(b) shows an optical micrograph after the first pass of TE ($\varepsilon_{ave} \approx 1.2$). The microstructure is heterogeneous with the peripheral areas more deformed than the central areas. Grains in the peripheral areas are mostly elongated and material flow is created due to the TE tool geometry. The central areas contain rather coarse grains, some of which appear equiaxed.

An optical micrograph after 4 passes of TE ($\varepsilon_{ave} \approx 4.8$) is shown in Fig. 2(c). The microstructure becomes finer with clear vortex flow of the material. The structure indicates that the billet underwent very high strain at the outer edge but less at the center. The microstructure appears as continuous development of the structure formed under the first TE pass.

The observation by optical microscopy reveals that the billet processed by TE has axial symmetry in microstructure. These observations of the macro-flow patterns are in qualitative agreement with the previous work,[15] although materials' structure-related specific features introduce minor differences. Indeed, investigation of microstructure in[15] was limited to representative, but separate areas, while this study has allowed to understand whole the cross-sectional macro-flow patterns.

EBSD analysis was then conducted at the center area (point A) and at the outer edge (point B) of the billets as marked in Fig. 1. Figure 3(a) and (b) show orientation images after one pass ($\varepsilon_{min} \approx 0.6$) and 4 passes ($\varepsilon_{min} \approx 2.4$) of TE at point A (center), respectively. The images reveal that a subgrain structure with low angle boundaries is well-

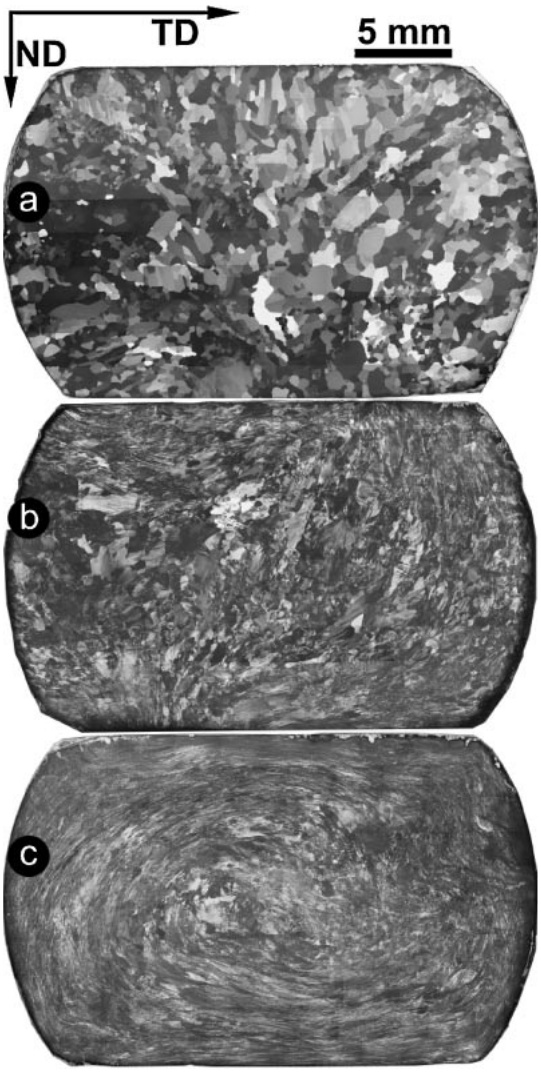

Fig. 2 Optical micrographs of cross-sections (a) before TE, (b) after one pass of TE and (c) after four passes of TE.

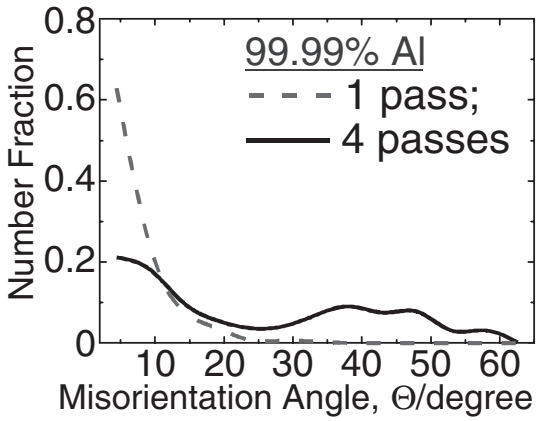

Fig. 4 Distribution of misorientation angle after one and four passes of TE at position A (center).

developed after one pass and this is essentially the same after 4 passes except that there are some grains with high angle boundaries in Fig. 3(b). This is demonstrated more clearly in Fig. 4 where the fraction of boundaries is plotted against misorientation angle. The fraction of low angle grain boundaries is large after one pass but it significantly decreases after 4 passes.

Orientation images after one pass ($\varepsilon_{max} \approx 2$) and 4 passes ($\varepsilon_{max} \approx 8$) of TE at point B (edge) are shown in Fig. 5(a) and (b), respectively. The microstructure consists of subgrains with low angle boundaries after one pass, but an alternate banded structure is developed after 4 passes with clear formation of fine grains surrounded by high angle boundaries. Figure 6 demonstrates more quantitatively the evolution of grain boundary structures from one pass to 4 passes: a significant decrease in low angle boundaries but instead a large increase in high angle boundaries is seen. When EBSD results are compared between point A and point B, the fraction of low angle boundaries is lowered and the overall fraction of high angle boundaries is higher at point B, that

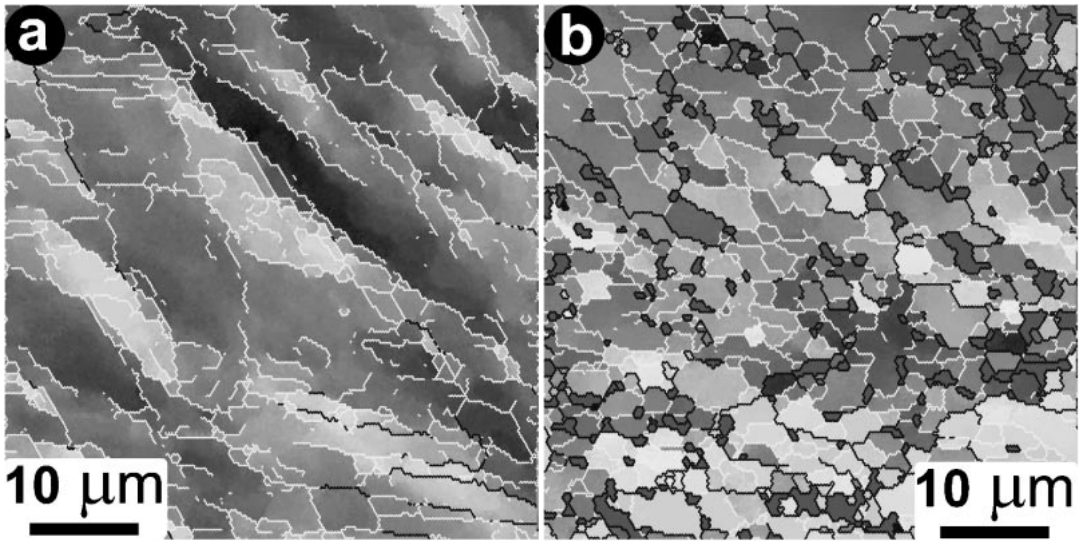

Fig. 3 Orientation images after one pass (a) and after four passes (b) of TE at point A (center). LABs ($2^\circ \leq \theta < 15^\circ$) are shown in white lines and HABs ($\theta \geq 15^\circ$) are shown in black lines. Grayscale contrast on the images corresponds to crystallographic orientations.

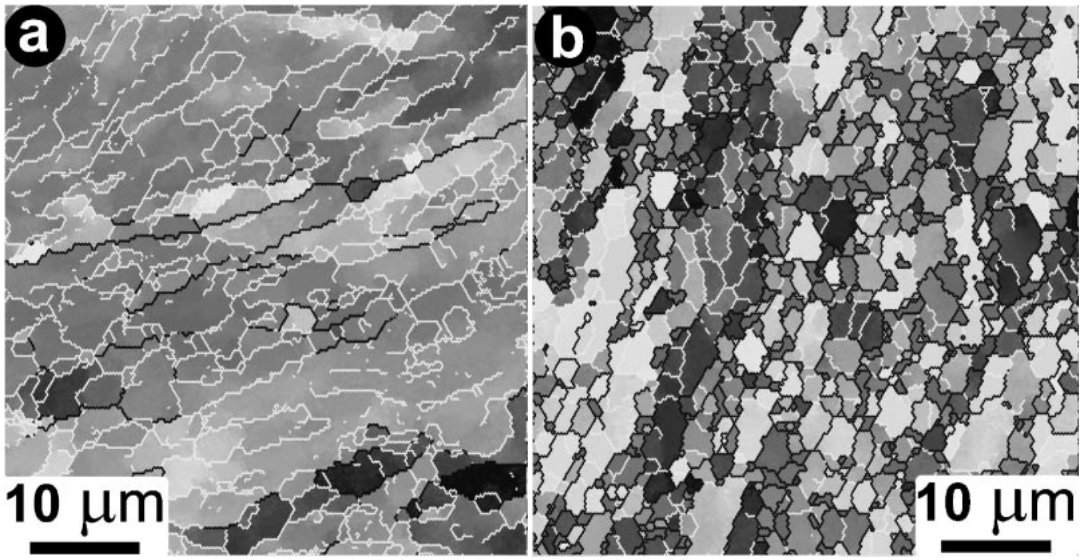

Fig. 5 Orientation images after one pass (a) and after four passes (b) of TE at point B (edge). LABs ($2^\circ \leq \theta < 15^\circ$) are shown in white lines and HABs ($\theta \geq 15^\circ$) are shown in black lines. Grayscale contrast on the images corresponds to crystallographic orientations.

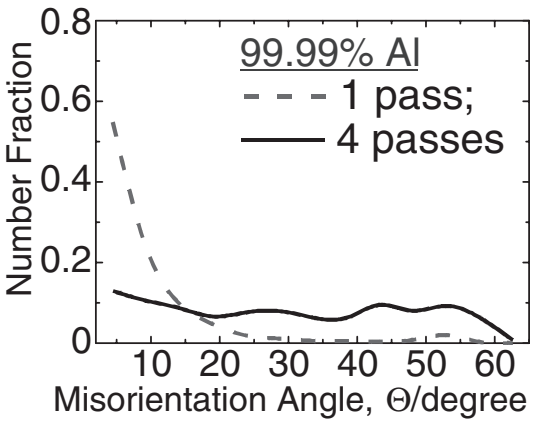

Fig. 6 Distribution of misorientation angle after one pass and four passes of TE at position B (edge).

rather well corresponds to the strain predicted by eqs. (1) and (2).

Summary of the EBSD analysis including (sub)grain size is given in Table 1. It is shown that the development of high angle boundaries is not sufficient after one pass but after 4 passes the fraction of high angle boundaries reaches more than 50% at point A and more than 70% at point B. When compared with quantitative results reported earlier for an Al-0.13%Mg alloy,[15] they are, again, in a good agreement qualitatively, but significantly different quantitatively. Namely, the fractions of HAB were limited only to 27% and 57% at the center and edge in the Al-Mg alloy even after 8 TE passes. This discrepancy should be attributed to substantial difference in dislocation structures between pure Al and Al-Mg. In pure Al, enhanced recovery reduces the accumulation of dislocations during the process but instead increases the fraction of HABs in the microstructure, while dynamic and static recovery is significantly inhibited by the dilute addition of Mg.

It is also shown that the grain size is reduced to $\sim$1.6 μm at point B after 4 passes of TE. This grain size is slightly larger than the ones obtained using the ECAP[22–24] and ARB[21] processes for the same grade of materials despite that all the ECAP, ARB and TE were conducted at room temperature. The difference might be attributed to a reversal character of straining under the TE processing. A similar effect was also observed in ECAP processing by route C. It should be noted that the process of route C in ECAP involves rotation of the billet by 180° about the longitudinal axis after each pass and thus reversal shear is introduced in the billet.[27] It should also be noted that route B_C has been used in ECAP process to obtain the finer grain sizes in previous reports,[22–24] where a billet is rotated by 90° between each pressing in the same sense so that different shear planes are activated to make the grain size finer.[27] These results show that structure evolution in TE of 99.99%Al is similar to all the SPD techniques previously reported and any of the SPD techniques is capable of providing an UFG structure. Main difference between these techniques is technological implementation. Thus, the TE technique has the following features and advantages:[16] size of distorted areas of the specimen, that is the head and rear parts, of the billet, is smaller under TE, which is especially important when doing repeated runs; (2) TE can maintain the initial shape of billets including those with an axial channel; (3) since TE does not change the direction of a billet's movement, it can be introduced into existing industrial lines by replacing a standard extrusion die with a twist extrusion die.

From the observations of this study, it is envisaged that, under TE operation, there may be two processes of structure evolution in 99.99%Al: first, development of the deformation-induced grain boundaries and second, a continuous increase in grain misorientations. Initially, the first process dominates, where the development of the deformation-induced boundaries occurs heterogeneously in the billet while directions of all boundaries are strongly affected by the tool geometry. The boundary spacing converges to a lower limit which is $\sim$1.6 μm for this study. Thereafter, the formation of new boundaries saturates and the second

process of a misorientation increase becomes dominant. LABs form on the first stages and continuously convert into HABs: namely, subgrain structures with low angle boundaries become grains with high angle boundaries. These observations are in a reasonable agreement with earlier results on microhardness and dislocation structure evolution reported in.[25)]

4. Summary and Conclusions

(1) High purity Al (99.99%) was processed by twist extrusion and microstructure evolution was analyzed using optical microscopy and electron backscattered diffraction analysis.

(2) After one pass of TE at average strain $\varepsilon_{ave} \approx 1.2$, the microstructure was heterogeneous with the peripheral areas more deformed than the central areas. Subgrain structures with low angle boundaries were developed throughout the cross section perpendicular to the longitudinal axis of the billet.

(3) After four passes of TE at strain level $\varepsilon_{ave} \approx 4.8$, a vortex-like material flow clearly appeared with axis symmetry and the microstructure consisted of grains with an increasing fraction of high angle boundaries: more than $\sim$50% at the center parts and more than $\sim$70% at the outer edge parts. The average grain size was reduced to $\sim$1.6 μm at the outer edge part after 4 passes of TE.

Acknowledgements

This work was supported in part by the Light Metals Educational Foundation of Japan; in part by the 21st COE program "Functional Innovation of Molecular Informatics" and Global COE program "Center of Excellence for Advanced Structural and Functional Materials Design", and in part by a Grant-in-Aid for Scientific Research in Priority Areas "Giant Straining Process for Advanced Materials Containing Ultra-High Density Lattice Defects", all from the Ministry of Education, Culture, Sports, Science and Technology, Japan.

REFERENCES

1) T. M. Osman, D. E. Rardon, L. B. Friedman and L. F. Vega: The Journal of Materials **58** (2006) 21–24.
2) T. C. Lowe: The Journal of Materials **58** (2006) 28–32.
3) R. Z. Valiev, Y. Estrin, Z. Horita, T. G. Langdon, M. J. Zehetbauer and Y. T. Zhu: The Journal of Materials **58** (2006) 33–39.
4) P. W. Bridgman: Studies in Large Plastic Flow and Fracture: With Special Emphasis on the Effects of Hydrostatic Pressure, (McGraw-Hill, New York, 1952).
5) V. M. Segal, V. I. Reznikov, A. E. Drobyshevkiy and V. I. Kopylov: Russian Metall (1981) 99.
6) V. M. Segal: Mater. Sci. Eng. A **197** (1995) 157–164.
7) G. A. Salishchev, O. R. Valiahmetov, R. M. Galeev and S. P. Malysheva: Izvestiya Akademii Nauk SSSR Metally (1996) 86–91.
8) J. Y. Huang, Y. T. Zhu, H. Jiang and T. C. Lowe: Acta Mater. **49** (2001) 1497–1505.
9) N. Tsuji, Y. Saito, H. Utsunomiya and S. Tanigawa: Scr. Mater. **40** (1999) 795–800.
10) Y. Saito, H. Utsunomiya, N. Tsuji and T. Sakai: Acta Mater. **47** (1999) 579–583.
11) Y. Beygelzimer, D. Orlov and V. Varyukhin: 2002 TMS Annual Meeting and Exhibition, ed. by Y. T. Zhu, T. G. Langdon, R. S. Mishra, S. L. Semiatin, M. J. Saran, T. C. Lowe., (TMS, Seattle, Washington, USA, 2002) pp. 297–304.
12) Y. Beygelzimer, V. Varyukhin, D. Orlov and S. Synkov: Twist extrusion–process for strain accumulation, (TEAN, Donetsk, 2003) p. 87.
13) Y. Y. Beygelzimer, V. N. Varyukhin, S. G. Synkov, A. N. Sapronov and V. G. Synkov: Physics and Technology of High Pressures **9** (1999) 109–110.
14) Y. Beygelzimer and D. Orlov: Defect and Diffusion Forum **208–209** (2002) 311–314.
15) M. Berta, D. Orlov and P. B. Prangnell: Inter. J. Mater. Res. **98** (2007) 200–204.
16) Y. Beygelzimer, D. Orlov, A. Korshunov, S. Synkov, V. Varyukhin, I. Vedernikova, A. Reshetov, A. Synkov, L. Polyakov and I. Korotchenkova: Solid State Phenomena **114** (2006) 69–78.
17) D. Orlov, A. Reshetov, A. Synkov, V. Varyukhin, D. Lotsko, O. Sirko, N. Zakharova, A. Sharovsky, V. Voropaiev, Y. Milman and S. Synkov: Twist Extrusion as a Tool for Grain Refinement in Al-Mg-Sc-Zr Alloys, ed. by Y. T. Zhu, V. Varyukhin vol 212, (Springer Netherlands, 2006) pp. 77–82.
18) V. V. Stolyarov, Y. E. Beigel'zimer, D. V. Orlov and R. Z. Valiev: The Physics of Metals and Metallography **99** (2005) 204–211.
19) D. V. Orlov, V. V. Stolyarov, H. S. Salimgareyev, E. P. Soshnikova, A. V. Reshetov, Y. Y. Beygelzimer, S. G. Synkov and V. N. Varyukhin: 2004 TMS Annual Meeting, ed. by Y. T. Zhu, T. G. Langdon, R. Z. Valiev, S. L. Semiatin, D. H. Shin, T. C. Lowe, (TMS, Charlotte, North Carolina, USA, 2004) pp. 457–462.
20) Y. Beygelzimer, V. Varyukhin, D. Orlov, B. Efros, V. Stolyarov and H. Salimgareyev: 2002 TMS Annual Meeting and Exhibition, ed. by Y. T. Zhu, T. G. Langdon, R. S. Mishra, S. L. Semiatin, M. J. Saran and T. C. Lowe, (TMS Seattle, Washington, USA, 2002) pp. 43–46.
21) N. Kamikawa, N. Tsuji, X. Huang and N. Hansen: Acta Mater. **54** (2006) 3055–3066.
22) Y. Iwahashi, Z. Horita, M. Nemoto and T. G. Langdon: Acta Mater. **46** (1998) 3317–3331.
23) S. D. Terhune, D. L. Swisher, K. Oh-ishi, Z. Horita, T. G. Langdon and T. R. McNelley: Metall. Mater. Trans. A **33A** (2002) 2173–2184.
24) A. P. Zhilyaev, D. L. Swisher, K. Oh-ishi, T. G. Langdon and T. R. McNelley: Mater. Sci. Eng. A **429** (2006) 137–148.
25) D. Orlov, Y. Beygelzimer, S. Synkov, V. Varyukhin and Z. Horita: Mater. Trans. **49** (2008) 2–6.
26) F. J. Humphreys: Scr. Mater. **51** (2004) 771–776.
27) M. Furukawa, Y. Iwahashi, Z. Horita, M. Nemoto and T. G. Langdon: Mater. Sci. Eng. A **257** (1998) 328–332.